

## Mu2e tracker momentum calibration using $\mu^- \longrightarrow e^- \bar{\nu}_e \nu_\mu$

Author:  
Tommaso Radicioni

Supervisor:  
Pasha Murat

Summer student programme 2015

# Contents

<b>1</b>	<b>Introduction</b>	<b>3</b>
1.1	Mu2e experiment . . . . .	3
1.1.1	Muon-to-electron conversion . . . . .	3
1.1.2	Mu2e apparatus overview . . . . .	4
1.1.3	Mu2e detector . . . . .	5
1.2	Mu2e tracker . . . . .	6
1.2.1	Tracker geometry . . . . .	6
1.2.2	Tracker resolution . . . . .	6
1.2.3	Calibration techniques . . . . .	7
<b>2</b>	<b>Analysis</b>	<b>9</b>
2.1	DIO electrons momentum parametrization and fit . . . . .	9
2.2	Strategy for the calibration run . . . . .	12
2.3	Summary and conclusions . . . . .	14

# Chapter 1

## Introduction

### 1.1 Mu2e experiment

#### 1.1.1 Muon-to-electron conversion

The goal of Mu2e experiment [1] is the search for the conversion of muons into electrons in the field of a nucleus of Al:

$$\mu^- + N \longrightarrow e^- + N \quad (1.1)$$

The expected signal is a mono-energetic electron with an energy equal to:

$$E_{\mu e} = m_\mu - E_b(Z) - R_N(A) = 104.97 \text{ MeV} \quad (1.2)$$

where  $E_b(Z) \simeq \frac{Z^2 \alpha^2 m_\mu}{2}$  is the nuclear recoil energy and  $R_N(A) \simeq \frac{m_\mu^2}{2m_N}$  is the atomic binding energy. Mu2e experiment intends to improve the single-event sensitivity (SES) on muon-to-electron conversion events which is planned to be  $R_{\mu e} \approx 2.5 \cdot 10^{-17}$  at 90% of confidence limit. The best experimental SES reached so far is  $R_{\mu e} < 7 \cdot 10^{-13}$  from SINDRUM II experiment so the order of magnitude of Mu2e improvement is  $10^4$  times. To achieve the sensitivity goal cited above, a high intensity, low energy muon beam coupled with a detector capable of efficiently identifying 105 MeV electrons while minimizing background from conventional processes will be required. At the proposed Mu2e sensitivity there are a number of processes that can mimic a muon-to-electron conversion signal. These backgrounds result principally from five sources:

- Intrinsic processes that scale with beam intensity and include muon decay-in-orbit (DIO) and radiative muon capture (RMC);
- Processes that are delayed because of particles that spiral slowly down the muon of a beamline, such as antiprotons;
- Prompt processes where the detected electron is nearly coincident in time with the arrival of a beam particle at the muon stopping target;
- Processes that mimic conversion electrons that are initiated by cosmic rays;

- Events that result from reconstruction errors induced by additional activity in the detector from conventional processes.

Decay-In-Orbit (DIO) electrons ( $\mu^- \text{Al} \rightarrow e^- \bar{\nu}_e \nu_\mu \text{Al}$ ) are the most important background. A free muon decays according to the Michel spectrum with a peak probability at the maximum energy at about half the muon rest energy (52.8 MeV) and far from the 105 MeV conversion electron energy. If the muon is bound in atomic orbit, the outgoing electron can exchange momentum with the nucleus, resulting in an electron with a maximum possible energy (ignoring the neutrino mass) equal to that of a Conversion Electron (CE), however with very small probability. At the kinematic limit of the bound decay, the two neutrinos carry away no momentum and the electron recoils against the nucleus, simulating the two-body final state of muon to electron conversion. The differential energy spectrum of electrons from muon Decay-In-Orbit falls rapidly as the energy approaches the endpoint, approximately as  $(E_{\text{endpoint}} - E_e)^5$ , and estimates of the spectrum near the CE energy  $E_{\mu e}$  vary by no more than 10%. The electron energy spectrum that results from muon decays in orbit in aluminum is illustrated in Figure 1.1 where the most prominent feature is the Michel peak:

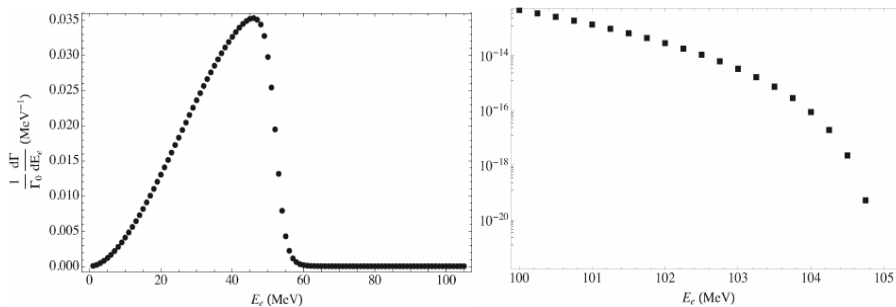


Figure 1.1: Electron energy spectrum from muons decaying in orbit from a 1s state in  $^{27}\text{Al}$ . Full range (left) and blowup of the endpoint (right).

### 1.1.2 Mu2e apparatus overview

Two proton batches, each containing  $4.0 \cdot 10^{12}$  protons with a kinetic energy of 8 GeV, are acquired from the Booster and injected into the Recycler Ring. A resonant extraction system injects every  $1.7 \mu\text{s}$  a bunch containing  $\approx 3 \cdot 10^7$  protons (called  $\mu\text{Bunch}$ ) into the external beamline. The proton pulses are delivered to the production target which is a radiatively cooled tungsten rod located in the evacuated warm bore of a high-field superconducting solenoid. The proton beam deflects in the magnetic field of the solenoid before striking the production target, complicating the final focus beamline optics and steering. The solenoid system is divided into 3 functional units derived from the Mu2e physics requirements:

- **Production Solenoid (PS):** a high field magnet with a graded solenoidal field varying smoothly from 4.6 T to 2.5 T. The PS is designed to capture pions and the muons into which they decay and guide them downstream to the TS.
- **Transport Solenoid (TS):** a S-shaped solenoid which consists of a set of superconducting solenoids and toroids that form a magnetic channel that

transmits low energy negatively charged muons from the PS to the DS. Positively charged particles and neutral particles are nearly all eliminated by absorbers and collimators before reaching the DS;

- **Detector Solenoid (DS):** a large and low field magnet that houses the muon stopping target and the components required to identify and analyze conversion electrons from the stopping target. The muon stopping target resides in a graded field that varies from 2 T to 1 T. The graded field captures conversion electrons that are emitted in the direction opposite the detector components causing them to reflect back towards the detector. The graded field also plays an important role in reducing background from high energy electrons that are transported to the Detector Solenoid by steadily increasing their pitch as they are accelerated towards the downstream detectors. The resulting pitch angle of these beam electrons is inconsistent with the pitch of a conversion electron from the stopping target.

The muon stopping target consists of a series of thin aluminum discs arranged coaxially along the DS axis. Energy loss and straggling in the stopping target are significant contributors to the momentum resolution function. The target is designed to stop as many muons as possible while minimizing the amount of material traversed by conversion electrons that are within the acceptance of the downstream tracker. The Mu2e detector is located inside the evacuated warm bore of the DS in a nearly uniform 1 Tesla magnetic field and is designed to efficiently and accurately identify and analyze the helical trajectories of  $\approx 10^5$  MeV electrons. The detector consists of a tracker and a calorimeter that provide redundant energy/momentum, timing, and trajectory measurements. A cosmic ray veto, consisting of both active and passive elements, surrounds the DS and nearly half of the TS. In the following picture, a schematic picture of the Mu2e apparatus is represented:

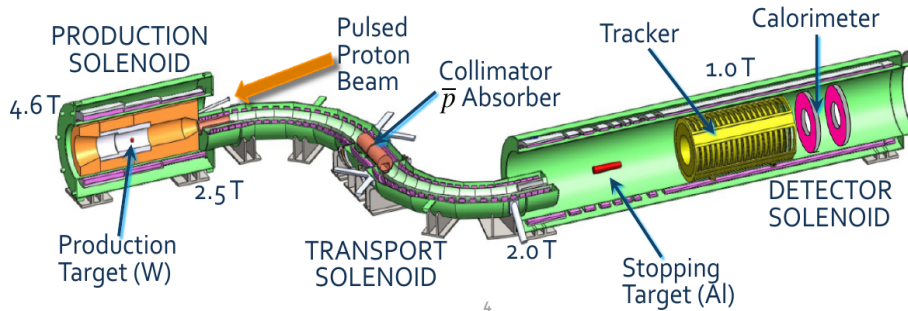


Figure 1.2: The Mu2e apparatus. The cosmic ray veto that surrounds the Detector Solenoid is not shown.

### 1.1.3 Mu2e detector

The Mu2e experiment must detect  $10^5 \frac{\text{MeV}}{c}$  electrons created in the Al stopping target with sufficiently good efficiency and resolution [2]. In order to measure signal events accurately, the Mu2e detector is composed of:

- a tracker, a low mass array of straw drift tubes aligned transverse to the axis of the DS. It is designed to accurately measure the trajectory

of electrons in a uniform 1 T magnetic field in order to determine their momenta;

- a calorimeter, 1860 BaF<sub>2</sub> crystals located downstream of the tracker and arranged in two disks which measure the electron energy, position and arrival time.

There are too many sources of  $\approx 100 \frac{MeV}{c}$  electrons to rely only on a calorimeter which only reports the existence of the particle and its energy. The calorimeter features doesn't allow the Mu2e experiment to separate efficiently electrons from the region of the stopping target from neutrons, photons, cosmic rays or any of a variety of sources with sufficient reliability and to get a sufficient energy resolution to reject electrons from the tail of DIO electrons distribution. For this reason, the success of the experiment depends critically on the tracker measurement.

## 1.2 Mu2e tracker

### 1.2.1 Tracker geometry

In order to solve the problems of high rate from the muon beam and make the vast majority of DIO invisible to the tracker, the tracker must be cylindrical with a central hole for passage of the remnant muon beam and background from DIO electrons. These DIO electrons curl in the solenoidal magnetic field of the detector with most of the spectrum executing helices with small radii. A  $52.8 \frac{MeV}{c}$  electron (the endpoint of the Michel spectrum for free muon decay) emitted with  $p_{\perp} = 52.8 \frac{MeV}{c}$  has a radius of 17.6 cm. The relevant equation to determine the inner and the outer radius of the tracker active region is  $p_{\perp} = 0.3qBR$ . A uniform solenoidal field equal to  $B=B_z=1$  T can be assumed in the following calculations. Since the stopping target radius is 6-10 cm and the maximum acceptance is for an angle  $\alpha$  of about  $60^{\circ}$  in the current field design, for an electron at  $p=105 \frac{MeV}{c}$  the inner radius is  $r_{inner} \approx \frac{p \sin 60^{\circ}}{0.3qB} + 10$  cm  $\approx 40$  cm. Moreover, considering that the diameter of the helix for a  $60^{\circ}$  pitch is 61 cm, the outer radius is  $\approx 70$  cm. For this reason, the active area of the tracker extends from about  $40 < r < 70$  cm (where radius  $r$  is measured from center of the muon beam). These dimensions have been optimized to maximize the acceptance ( $\approx 20\%$  excluding track quality cuts) to CEs while minimizing the number of low energy electrons that intersect the tracker. As the measurement of the electron momentum in the tracker is the primary Mu2e measurement, the tracker calibration and the determination of its intrinsic momentum resolution are fundamental.

### 1.2.2 Tracker resolution

The determination of the CE momentum is degraded by energy loss in the stopping target and proton absorber before the electron reaches the tracker. After stochastic effects are included, a signal distribution is seen with a FWHM  $\approx 800 \frac{keV}{c}$ , or  $\sigma \approx 350 \frac{keV}{c}$ . For this reason, the tracker resolution is required to be small on this scale so that it doesn't significantly contribute to the width of the signal momentum measurement. Monte Carlo simulations tell us the

momentum resolution of the electrons has a high-side resolution of  $\sigma \approx 120 \frac{keV}{c}$ . The requirement on the low-side tail is much less stringent since it only causes acceptance loss of the signal and it smears DIO background away from the signal region. Figure 1.3 shows the resolution function for an electron entering the tracker:

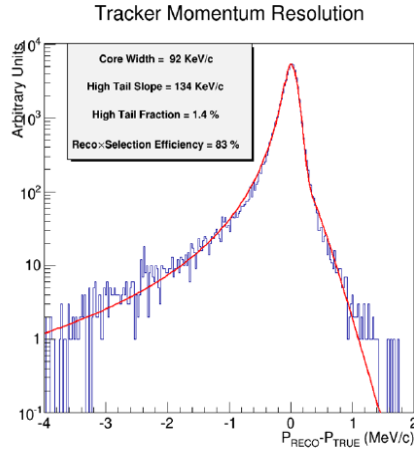


Figure 1.3: Conversion electron momentum resolution. Fit to a split double Gaussian with standard track fit quality cuts.

If the low-side resolution is much larger than shown, the CEs excessively smear into the DIO region and spoil the acceptance; if the high-side core resolution is much larger than  $200 \frac{keV}{c}$ , an unacceptable number of DIO electrons smear into the signal region just from Gaussian smearing. Current simulated resolutions imply acceptable background levels.

### 1.2.3 Calibration techniques

The tracker calibration accuracy ultimately limits the accuracy of the DIO background rate estimate. The tracker calibration precision, together with smearing effects, set the limit for the precision of the DIO background estimate. Indeed, the shape of both the DIO and signal depends strongly on non-zero values of momentum scale and shift. The accuracy and precision of the DIO background rate estimate dominate the estimate of the Mu2e conversion signal sensitivity. In order to calibrate the tracker momentum response, a source of particles with known momentum is needed. The most promising options are the following[3][4][5]:

- measurement of the mono-energetic peak of electrons at  $\approx 67 \frac{MeV}{c}$  from  $\pi^+ \rightarrow e^+ \bar{\nu}_e$  decays of pions stopped in the stopping target. The tracker acceptance for this calibration process is optimized at the DS field of about 0.7 T. Moreover, a dedicated run with a reversed charge selection (obtained through the collimator rotation in the TS), a time window change and a reduction of the beam intensity is needed. This calibration implies many difficulties since the signal is very small ( $BR(\pi^+ \rightarrow e^+ \bar{\nu}_e) \approx 10^{-4}$  and

only  $10^{-6}\pi^+$  per Proton On Target (POT) are observed) and since there are a number of processes that can mimic the  $\pi^+$  decay in the  $e^+$  channel;

- reconstruction of the DIO electrons spectrum edge from  $\mu^- \rightarrow e^- \bar{\nu}_e \nu_\mu$ . The optimal magnetic field for this calibration is close to 0.5 T due to the tracker acceptance. A dedicated with a reduced proton intensity is needed;
- reconstruction of the Michel spectrum edge of electrons at  $52.8 \frac{MeV}{c}$  from  $\mu^+ \rightarrow e^+ \nu_e \bar{\nu}_\mu$ . In this calibration, the momentum edge is much sharper wrt the previous case but, in addition to a reduced proton intensity, a reversed charge selection through the collimator rotation in the TS is needed. Moreover, in order to achieve the same acceptance as CEs, the field would need to be reduced at 0.5 T;
- electrons and muons produced by the cosmic rays in the detector material which are reconstructed in the tracker both upstream and downstream. Reflecting particles are reconstructed as two separate tracks, once on their upstream path and again on the downstream. The difference in the reconstructed momentum values of these tracks can be fit to extract the momentum resolution and shift, over a broad range of momenta, angles, and positions in the tracker. This calibration can be done at the nominal magnetic field value equal to 1 T.

In the following analysis, the reconstruction of the DIO electrons spectrum from  $\mu^- \rightarrow e^- \bar{\nu}_e \nu_\mu$  has been taken into account and studied in order to determine the feasibility and the accuracy of this source of calibration.

# Chapter 2

## Analysis

### 2.1 DIO electrons momentum parametrization and fit

Assuming that the reconstructed value of the curvature ( $c_{reco}$ ) is close to the true one ( $c_{true}$ ), the value of  $c_{reco}$  can be expressed as a Taylor expansion of  $c_{true}$ :

$$c_{reco} = c_{true} + \alpha c_{true} + \beta + \dots \quad (2.1)$$

where the parameter  $\beta$  is called *false curvature* and the parameter  $\alpha$  is called *absolute momentum scale*. The former is a constant parameter and it could be non-zero because of a tracker misalignment whereas the latter is proportional to  $c_{true}$  and it is due to a hypothetical slight difference in the expected magnetic field value wrt the true value ( $B_{exp}=(1-\alpha)B_{true}$ ). The effect of a non-zero  $\alpha$  value is shown in Figure 2.1 where  $\alpha$  is imposed to be equal to  $\alpha=0.1$ :

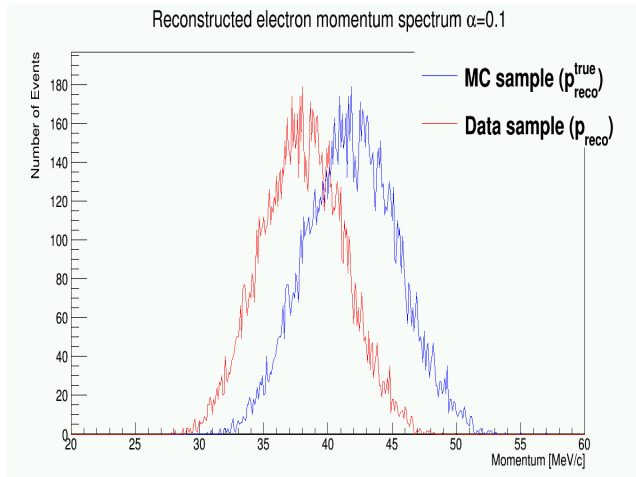


Figure 2.1: Reconstructed electrons momentum spectrum with  $\alpha=0$  ( $p_{reco}^{true}$ ) and with  $\alpha=0.1$  ( $p_{reco}$ )

Momentum resolution due to fluctuations of the electron energy losses is about  $300\text{-}350\frac{\text{keV}}{c}$  so systematic uncertainties in the tracker momentum reconstruction must be small compared to that. This leads to the requirement for the absolute momentum scale to be calibrated with an accuracy of  $0.1\%$  ( $\approx 100\frac{\text{keV}}{c}$ ). In the following analysis, the false curvature has been considered negligible so that a study of the effect of a non-zero momentum scale value has been performed. First of all, two samples of DIO events have been generated using the same generator code. Those samples are called **Monte Carlo sample** and **Simulated data sample**. The difference between those two samples are the following:

- **events statistics:**  $10^6$  MC events have been generated whereas the number of simulated data events is equal to  $2.5 \cdot 10^5$  events. Thus, statistical error in MC sample is not a limitation factor for the following analysis;
- **magnetic field:** magnetic field value in simulated data sample is  $0.5\%$  lower wrt MC samples so that an  $\alpha$  value different from zero has been simulated. In particular, in this analysis the simulated  $\alpha$  value is  $\alpha=0.005$ .

In Figure 2.2, reconstructed DIO electrons momentum is reported after that a set of fit quality requirement for reconstructed tracks has been applied:

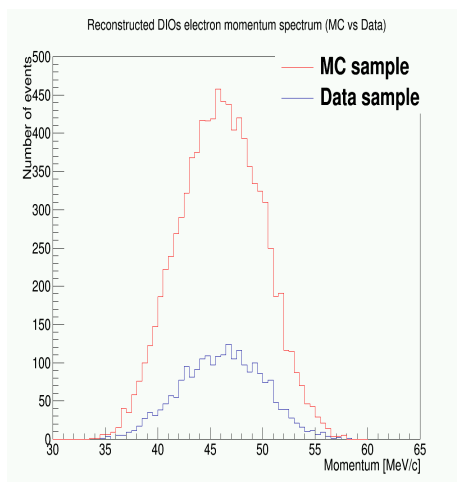


Figure 2.2: Reconstructed DIO electrons momentum in MC sample and simulated data sample

In order to fit the reconstructed momentum spectrum for DIO electrons in the MC sample, a piecewise function, called  $f(p)$  and represented in Figure 2.3, has been defined in three different intervals of momentum values in the following way:

- a parabola  $a_i + b_i \cdot x + c_i \cdot x^2$  ( $i=1,2,3$ ), where  $a_i$ ,  $b_i$  and  $c_i$  are free parameters, is plotted in each interval after the parameters have been deduced by the fit;
- a linear interpolation has been realized in order to connect smoothly two next function regions.

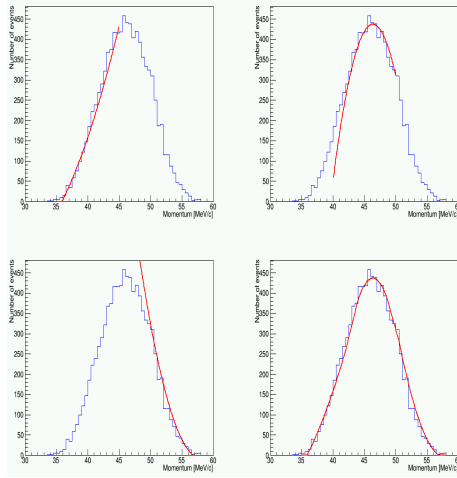


Figure 2.3: In the top left, top right and bottom left pictures single parabolas are represented. In the bottom right picture, the final function  $f(p)$  is represented after smooth connections between plot regions have been realized

This fit technique has an important advantage: since it's not sensitive to the statistical jitter, it's possible to implement this technique for a huge class of functions in order to use accurate analytical approximation for histograms which are usually affected by fluctuations. After all  $f(p)$  parameters are fixed, it's possible to fit the reconstructed DIO electrons momentum spectrum in simulated data sample using a function  $F(p)=N \cdot f((1 + \alpha)p)$ , where  $N$  is a normalization factor and  $\alpha$  is the absolute momentum scale and they are both free parameters. The fit result is shown in Figure 2.4:

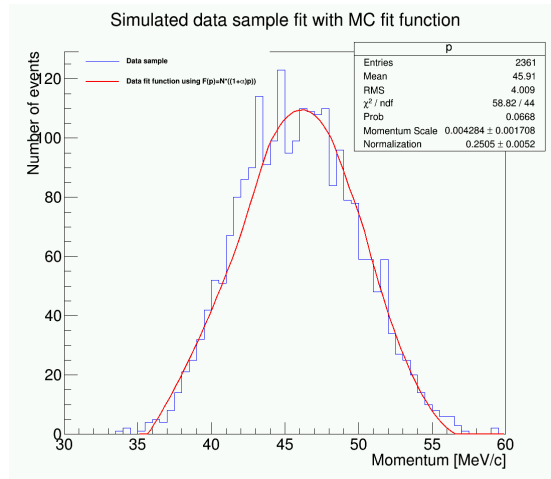


Figure 2.4: Fit result using  $F(p)$  in simulated data sample

As it is possible to observe in the right panel of the picture, value returned

by the fit is  $\alpha=0.004284\pm 0.001708$  compatible within the statistical accuracy with the expected value equal to  $\alpha=0.005$ . Moreover, the normalization factor is  $N=0.2505\pm 0.0052$  which is coherent with the difference in the events statistics for the generated samples. In order to reach the required accuracy is needed 4 times the number of simulated data events.

## 2.2 Strategy for the calibration run

At nominal proton beam intensity, the expected number of DIO electrons is  $\approx 2 \cdot 10^4$  per  $\mu$ Bunch. At 1 T, most of DIO electrons doesn't produce hits in the detector since they go in the central hole of the tracker so a reduction of the magnetic field value up to 0.5 T is needed to detect the spectrum edge. At half field,  $\approx 5 \cdot 10^3$  electrons per  $\mu$ Bunch are in the acceptance band of the tracker, as shown in Figure 2.5:

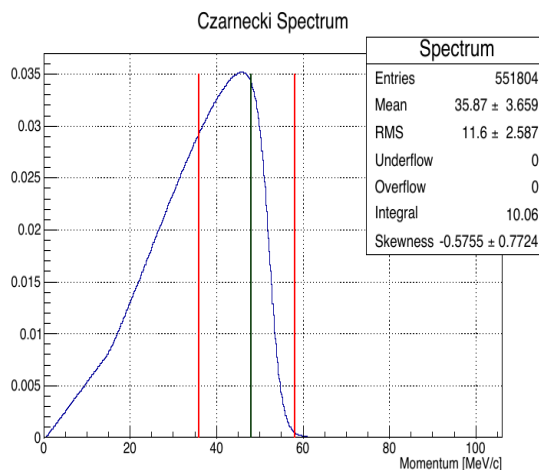


Figure 2.5: The acceptance band of the tracker lies between the two red lines represented in the figure

Without a reduced proton intensity, DIO electrons hit multiple times inner straw tubes causing misreconstruction effects. For this reason, a reduction of DIO electrons per  $\mu$ Bunch is needed in order to improve the momentum reconstruction. The number of protons per bunch could be reduced by a factor of about 10. The stability of the accelerator control system could be affected by increasing the reduction factor beyond that value. Moreover, an additional reduction of  $10 \div 100$  could be achieved by moving and defocusing the extracted proton beam before the production target. If a reduction factor of  $\approx \frac{1}{1000}$  had applied to the proton intensity, the expected number of DIO electrons per  $\mu$ Bunch would be  $\approx 5$ . Finally, data acquisition timing has been studied in order to find out if there could be difficulties in reading and writing the disk array during the calibration run. The flow of signals through the readout chain is shown in Figure 2.6:

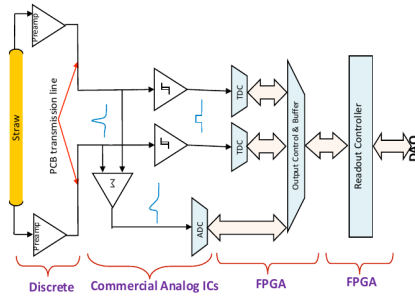


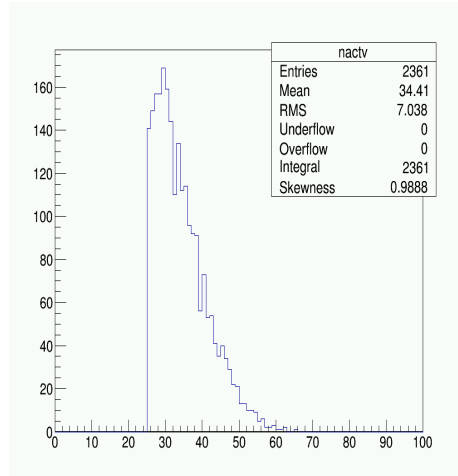
Figure 2.6: Signal flow through front end electronics.

Assuming that no online triggering is needed and all events taken during the calibration run are written to disk, the bandwidth  $B$  required for a calibration run at 0.5 T is given by the following formula:

$$B = N\left(\frac{\text{Bytes}}{\text{hits}}\right)N\left(\frac{\text{hits}}{\mu\text{Bunch}}\right)N\left(\frac{\mu\text{Bunch}}{s}\right) \quad (2.2)$$

to be compared with the maximum data logger rate to read and write the disk array equal to  $B \approx 50 \frac{MB}{s}$ . All the values of the factors of the formula in Equation 2.2 are reported here below:

- DAQ system transfer data at 128 bits per hit format, that is  $N\left(\frac{\text{Bytes}}{\text{hits}}\right) = 16 \frac{\text{Bytes}}{\text{hits}}$ ;
- the mean number of hits per  $\mu\text{Bunch}$  is  $\approx 35$  as shown in Figure 2.7;
- the number of  $\mu\text{Bunch}$  per second is  $\approx 2 \cdot 10^5$ .

Figure 2.7: Mean number of hits per  $\mu\text{Bunch}$  in simulated data sample

Putting those numbers in Equation 2.2, the estimated value of the bandwidth for the calibration run is  $B \approx 100 \frac{MB}{s}$  so it is possible to conclude that  $\approx 0.5$  DIO electrons per  $\mu\text{Bunch}$  allows us to efficiently transfer data.

## 2.3 Summary and conclusions

Mu2e experiment could employ multiple calibration techniques to calibrate the tracker and establish the DIO background to the conversion signal in a convincing, complete and consistent way. The possibility to use reconstructed DIO electrons spectrum to calibrate tracker has been studied and the fit results suggest that a non-zero momentum scale value is predictable by using an approximated function. At half field, a reduced proton intensity is needed to prevent misreconstruction effects and DAQ system difficulties. The maximal beam intensity value for the dedicated run is a parameter to be determined before the calibration in order to improve the events reconstruction in the tracker and to transfer data efficiently. Effects due to a non-zero false curvature value have still to be studied and combined with the results reported in this analysis. Finally, advantages of other calibration sources have to be studied in terms of accuracy and feasibility in order to obtain a complete overview before the calibration run.

# Bibliography

- [1] Mu2e collaboration, *Mu2e Technical Design Report*, October 2014: Fermi National Accelerator Laboratory Batavia, IL 60510.
- [2] R. Bernstein A. Mukherjee, *Tracker Requirements Document*, 19 March 2014, Mu2e internal note, Mu2e-doc-732-v20.
- [3] D. Brown. *Calibration Overview*, 15 April 2015, Mu2e internal note, Mu2e-doc-5392-v2.
- [4] M. Chiappini P. Murat, *Using DIO  $\mu^- \rightarrow e^- \bar{\nu}_e \nu_\mu$  Decays for Tracker Calibration*, 24 October 2014, Mu2e internal note, Mu2e-doc-4614-v1.
- [5] D. Brown D. Glenzinski J. Miller *Mu2e Tracker Calibration Plan*, 6 July 2015, Mu2e internal note, Mu2e-doc-5813-v1.